Eur. Phys. J. C 17, 695–706 (2000)
Digital Object Identifier (DOI) 10.1007/s100520000511

THE EUROPEAN PHYSICAL JOURNAL C

Leptoquark signal from global analysis

A.F. Żarnecki

Institute of Experimental Physics, Warsaw University, Hoża 69, 00-681 Warszawa, Poland (e-mail: zarnecki@fuw.edu.pl)

Received: 21 June 2000 / Revised version: 31 August 2000 /
Published online: 23 October 2000 – © Springer-Verlag 2000

Abstract. Data from HERA, LEP and the Tevatron as well as from low energy experiments are used to constrain the Yukawa couplings for scalar and vector leptoquarks in the Buchmüller–Rückl–Wyler effective model. In the limit of very high leptoquark masses constraints on the coupling to the mass ratio λ/M are derived using the contact-interaction approximation. For finite masses the coupling limits are studied as a function of the leptoquark mass. Some leptoquark models are found to describe the existing experimental data much better than the standard model. The increase in the global probability observed for models including S_1 or $\tilde{V}_0$ leptoquark production/exchange corresponds to an effect of more than 3σ. Assuming that a real leptoquark signal is observed, the allowed region in the λ–M plane is calculated. The leptoquark signal mostly results from the new data on the atomic parity violation in cesium, but is also supported by recent LEP2 measurements, unitarity violation in the CKM matrix and HERA high-Q^2 results.

1 Introduction

In 1997 the H1 [1] and ZEUS [2] experiments at HERA reported an excess of events in positron–proton neutral current deep inelastic scattering (NC DIS) at very high momentum transfer scales Q^2, as compared with the predictions of the standard model. As a possible sign of some "new physics" these results provoked many theoretical speculations. Clustering of H1 events at positron-jet invariant masses of about 200 GeV was considered to indicate the possible resonant production of leptoquark states. The agreement with the standard model prediction improved after both experiments doubled their positron–proton data samples, but some discrepancy is still there and calls for a better understanding.

In a paper presented last year [3][1], data from HERA, LEP and the Tevatron as well as from low energy experiments were used to constrain the mass scale of the possible new electron–quark contact interactions. A contact-interaction model was used as the most general framework which can describe possible low energy effects coming from "new physics" at much higher energy scales. This includes the possible existence of second-generation heavy weak bosons, leptoquarks as well as electron and quark compositeness [5,6]. In addition to the general models, in which all new contact-interaction couplings can vary independently, the global analysis considered also a set of one-parameter models which assumed fixed relations between the couplings. However, only parity conserving models were selected, as suggested by ZEUS [7], to avoid strong limits coming from atomic parity violation (APV) measurements [8]. No significant improvement in the description of the data has been obtained for any of these models.

Theoretical uncertainties in the parity violation measurements in cesium atoms recently have significantly been reduced. As a result, the measured value of the cesium weak charge is now more than 2σ away from the standard model predictions [9]. This discrepancy could be due to new parity-violating electron–quark interactions. Considered in this paper are effects induced by the possible existence of the first-generation leptoquarks. Predictions based on the Buchmüller–Rückl–Wyler (BRW) effective model [10] are compared with the existing experimental data. In the limit of very high masses, the exchange of leptoquarks can be described using the contact-interaction approach [11]. Limits on the ratio of the coupling and the mass are derived. For finite leptoquark masses limits on leptoquark Yukawa coupling λ are studied as a function of the leptoquark mass.

The aim of the present analysis is to combine the APV measurements with other data to constrain the leptoquark coupling and mass, and to look for a possible leptoquark signal in the combined data. The BRW model used in this analysis is described in Sect. 2. In Sect. 3 the relevant data from HERA, LEP, the Tevatron and other experiments are briefly described. Methods used to compare data with leptoquark model predictions and to derive coupling limits are summarized in Sect. 4. The results of the analysis for different leptoquark types, including the extracted coupling-mass limits and a discussion of the possible leptoquark signal are presented in Sect. 5.

The analysis presented here is based on the approach used in the global analysis of $eeqq$ contact interactions

[1] For a recent update of the results presented see [4]

[3,4], which in turn followed [12,13]. When finalizing this analysis another work discussing leptoquark exchange as a possible explanation for the APV result was released [14]. However, the analysis presented there is limited to the contact-interaction approximation.

2 Leptoquark models

The striking symmetry between quarks and leptons in the standard model strongly suggests that, if there exists a more fundamental theory it should also introduce a more fundamental relation between them. Such a lepton–quark "unification" is achieved for example in different theories of grand unification [15] and in compositeness models. Whenever quarks and leptons are allowed to couple directly to each other, a quark–lepton bound state can also exist. Such particles, called leptoquarks, carry both color and fractional electric charge and a lepton number. Also supersymmetric theories with broken R-parity predict squarks (leptoquark type objects) coupling to quark–lepton pairs.

In this paper a general classification of leptoquark states proposed by Buchmüller, Rückl and Wyler [10] will be used. The Buchmüller–Rückl–Wyler (BRW) model is based on the assumption that new interactions should respect the $SU(3)_C \times SU(2)_{\rm L} \times U(1)_Y$ symmetry of the standard model. In addition leptoquark couplings are assumed to be family diagonal (to avoid FCNC processes) and to conserve lepton and baryon numbers (to avoid rapid proton decay). Taking into account very strong bounds from rare decays it is also assumed that leptoquarks couple either to left- or to right-handed leptons. With all these assumptions there are 14 possible states (isospin singlets or multiplets) of scalar and vector leptoquarks. Table 1 lists these states according to the so-called Aachen notation [16]. An S (V) denotes a scalar (vector) leptoquark and the subscript denotes the weak isospin. When the leptoquark can couple to both right- and left-handed leptons, an additional superscript indicates the lepton chirality. A tilde is introduced to differentiate between leptoquarks with different hypercharges. Listed in Table 1 are the leptoquark fermion number F, electric charge Q, and the branching ratio to an electron–quark pair (or electron–antiquark pair), β. The leptoquark branching fractions are predicted by the BRW model and are either 1, 1/2 or 0. For a given electron–quark branching ratio β, the branching ratio to the neutrino–quark is by definition $(1-\beta)$. Also included in Table 1 are the flavors and chiralities of the lepton–quark pairs coupling to a given leptoquark type. In three cases the squark flavors (in supersymmetric theories with broken R-parity) with corresponding couplings are also indicated. The present analysis takes into account only leptoquarks which couple to the first-generation leptons (e, ν_e) and first-generation quarks (u, d), as most of the existing experimental data constrain this type of couplings. Second- and third-generation leptoquarks as well as generation-mixing leptoquarks will not be considered in this paper. It is also assumed that one of the leptoquark types gives the dominant contribution, as compared with other leptoquark states and that the interference between different leptoquark states can be neglected. Using this simplifying assumption, different leptoquark types can be considered separately. Finally, it is assumed that different leptoquark states within isospin doublets and triplets have the same mass.

Table 1. A general classification of leptoquark states in the Buchmüller–Rückl–Wyler model. Listed are the leptoquark fermion number, F, electric charge, Q (in units of elementary charge), the branching ratio to electron–quark (or electron–antiquark) pairs, β, and the flavors of the coupled lepton–quark pairs. Also shown are possible squark assignments to the leptoquark states in the minimal supersymmetric theories with broken R-parity

Model	Fermion number F	Charge Q	BR(LQ $\to e^{\pm}q$) β	Coupling		Squark type
$S_0^{\rm L}$	2	$-1/3$	1/2	$e_{\rm L}u$	νd	$\tilde{d}_R$
$S_0^{\rm R}$	2	$-1/3$	1	$e_{\rm R}u$		
$\tilde{S}_0$	2	$-4/3$	1	$e_{\rm R}d$		
$S_{1/2}^{\rm L}$	0	$-5/3$	1	$e_{\rm L}\bar{u}$		
		$-2/3$	0		$\nu\bar{u}$	
$S_{1/2}^{\rm R}$	0	$-5/3$	1	$e_{\rm R}\bar{u}$		
		$-2/3$	1	$e_{\rm R}\bar{d}$		
$\tilde{S}_{1/2}$	0	$-2/3$	1	$e_{\rm L}\bar{d}$		$\overline{\tilde{u}_{\rm L}}$
		$+1/3$	0		$\nu\bar{d}$	$\overline{\tilde{d}_{\rm L}}$
S_1	2	$-4/3$	1	$e_{\rm L}d$		
		$-1/3$	1/2	$e_{\rm L}u$	νd	
		$+2/3$	0		νd	
$V_0^{\rm L}$	0	$-2/3$	1/2	$e_{\rm L}\bar{d}$	$\nu\bar{u}$	
$V_0^{\rm R}$	0	$-2/3$	1	$e_{\rm R}\bar{d}$		
$\tilde{V}_0$	0	$-5/3$	1	$e_{\rm R}\bar{u}$		
$V_{1/2}^{\rm L}$	2	$-4/3$	1	$e_{\rm L}d$		
		$-1/3$	0		νd	
$V_{1/2}^{\rm R}$	2	$-4/3$	1	$e_{\rm R}d$		
		$-1/3$	1	$e_{\rm R}u$		
$\tilde{V}_{1/2}$	2	$-1/3$	1	$e_{\rm L}u$		
		$+2/3$	0		νu	
V_1	0	$-5/3$	1	$e_{\rm L}\bar{u}$		
		$-2/3$	1/2	$e_{\rm L}\bar{d}$	$\nu\bar{u}$	
		$+1/3$	0		$\nu\bar{d}$	

The ep collider HERA is the unique place to search for the first-generation leptoquarks, as single leptoquarks can directly be produced in electron–quark interactions. The influence of the leptoquark production or exchange on the ep NC DIS cross section can be described as an additional term in the tree level $eq \to eq$ scattering amplitude[2]:

$$M_{ij}^{eq}(s,t,u) = -\frac{4\pi\alpha_{\rm em}e_q}{t} + \frac{4\pi\alpha_{\rm em}}{\sin^2\theta_{\rm W}\cos^2\theta_{\rm W}} \cdot \frac{g_i^e g_j^q}{t-M_Z^2} + \eta_{ij}^{eq}(s,u), \quad (1)$$

[2] The amplitude given for electron–quark scattering describes also scattering of positrons and anti-quarks taken with opposite chiralities

Table 2. Coefficients a_{ij}^{eq} defining the effective contact-interaction couplings $\eta_{ij}^{eq} = a_{ij}^{eq} \cdot \lambda_{\rm LQ}^2/M_{\rm LQ}^2$ for different models of scalar (upper part of the table) and vector (lower part) leptoquarks. Empty places in the table correspond to $a_{ij}^{eq} = 0$

Model	$a_{\rm LL}^{ed}$	$a_{\rm LR}^{ed}$	$a_{\rm RL}^{ed}$	$a_{\rm RR}^{ed}$	$a_{\rm LL}^{eu}$	$a_{\rm LR}^{eu}$	$a_{\rm RL}^{eu}$	$a_{\rm RR}^{eu}$
$S_0^{\rm L}$					$+1/2$			
$S_0^{\rm R}$								$+1/2$
$\tilde{S}_0$				$+1/2$				
$S_{1/2}^{\rm L}$						$-1/2$		
$S_{1/2}^{\rm R}$			$-1/2$				$-1/2$	
$\tilde{S}_{1/2}$		$-1/2$						
S_1	$+1$				$+1/2$			
$V_0^{\rm L}$	-1							
$V_0^{\rm R}$				-1				
$\tilde{V}_0$								-1
$V_{1/2}^{\rm L}$		$+1$						
$V_{1/2}^{\rm R}$			$+1$				$+1$	
$\tilde{V}_{1/2}$						$+1$		
V_1	-1				-2			

where s, t and u are the Mandelstam variables describing the electron–quark scattering subprocess, e_q is the electric charge of the quark in units of the elementary charge, the subscripts i and j label the chiralities of the initial lepton and quark, respectively ($i, j = {\rm L}, {\rm R}$), and g_i^e and g_j^q are the electroweak couplings of the electron and the quark. In the limit $M_{\rm LQ} \gg s^{1/2}$ the leptoquark contribution to the scattering amplitude given by $\eta_{ij}^{eq}(s,u)$ does not depend on the process kinematics and can be written as

$$\eta_{ij}^{eq} = a_{ij}^{eq} \cdot \left(\frac{\lambda_{\rm LQ}}{M_{\rm LQ}}\right)^2, \qquad (2)$$

where $M_{\rm LQ}$ is the leptoquark mass, $\lambda_{\rm LQ}$ the leptoquark–electron–quark Yukawa coupling and the coefficients a_{ij}^{eq} are given in Table 2 [11]. The effect of heavy leptoquark production or exchange is equivalent to a vector type $eeqq$ contact interaction. It is interesting to notice that 5 scalar leptoquark types ($S_0^{\rm R}$, $\tilde{S}_0$, $S_{1/2}^{\rm L}$, $S_{1/2}^{\rm R}$ and $\tilde{S}_{1/2}$) correspond to the same contact-interaction coupling structures (but opposite coupling signs) as 5 vector models ($\tilde{V}_0$, $V_0^{\rm R}$, $\tilde{V}_{1/2}$, $V_{1/2}^{\rm R}$ and $V_{1/2}^{\rm L}$ respectively).

For leptoquark masses comparable with the available ep center-of-mass energy the u-channel leptoquark exchange process and the s-channel leptoquark production have to be considered separately. Corresponding diagrams for $F = 0$ and $F = 2$ leptoquarks are shown in Fig. 1. The leptoquark contribution to the scattering amplitude can now be described by the following formulae:

(1) for u-channel leptoquark exchange ($F = 0$ leptoquark in e^-q or $e^+\bar{q}$ scattering, or $|F| = 2$ leptoquark in e^+q or $e^-\bar{q}$ scattering)

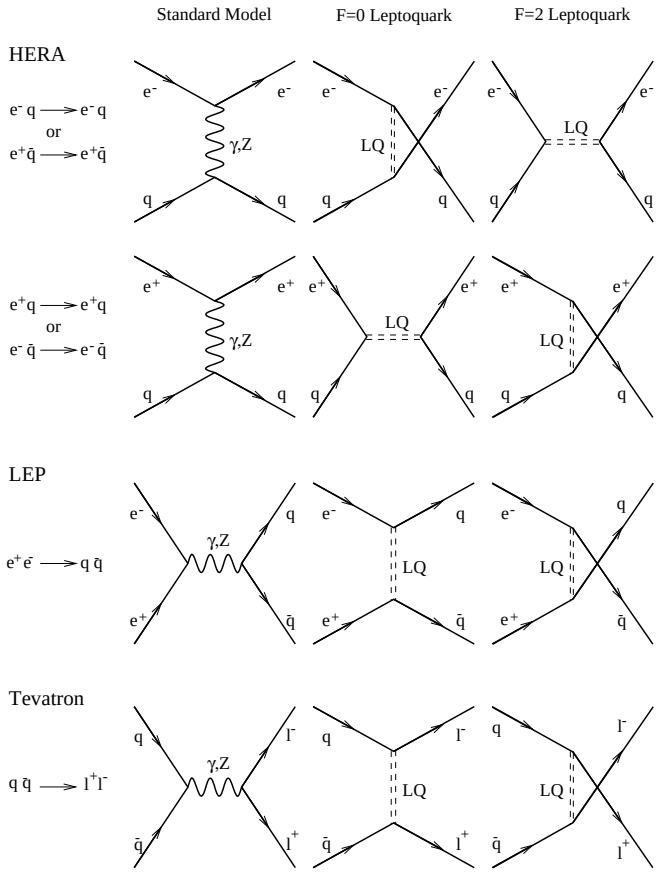

Fig. 1. Diagrams describing leading-order standard model processes and leptoquark contributions coming from $F = 0$ and $F = 2$ leptoquarks, for NC DIS at HERA, quark-pair production cross section at LEP and Drell–Yan process at the Tevatron, as indicated in the plot

$$\eta_{ij}^{eq}(s,u) = \frac{a_{ij}^{eq} \cdot \lambda_{\rm LQ}^2}{M_{\rm LQ}^2 - u},$$

(2) for s-channel leptoquark production ($F = 0$ leptoquark in e^+q or $e^-\bar{q}$ scattering, or $|F| = 2$ leptoquark in e^-q or $e^+\bar{q}$ scattering)

$$\eta_{ij}^{eq}(s,u) = \frac{a_{ij}^{eq} \cdot \lambda_{\rm LQ}^2}{M_{\rm LQ}^2 - s - {\rm i}s\frac{\Gamma_{\rm LQ}}{M_{\rm LQ}}},$$

where $\Gamma_{\rm LQ}$ is the total leptoquark width. The partial decay width for every decay channel is given by the formula

$$\Gamma_{\rm LQ} = \frac{\lambda_{\rm LQ}^2 M_{\rm LQ}}{8\pi(J+2)},$$

where J is the leptoquark spin.

For processes such as $e^+e^- \to$ hadrons a corresponding formula can be written for the $e^+e^- \to q\bar{q}$ tree level amplitude:

$$M_{ij}^{ee}(s) = -\frac{4\pi\alpha_{\rm em}e_q}{s} + \frac{4\pi\alpha_{\rm em}}{\sin^2\theta_{\rm W}\cos^2\theta_{\rm W}} \cdot \frac{g_i^e g_j^q}{s - M_Z^2 + {\rm i}s\frac{\Gamma_Z}{M_Z}} + \eta_{ij}^{eq}(t,u), \qquad (3)$$

where the subscripts i and j label the chiralities of the initial lepton and final quark respectively and

$$\eta_{ij}^{eq}(t,u) = \begin{cases} \dfrac{a_{ij}^{eq}\cdot\lambda_{\rm LQ}^2}{M_{\rm LQ}^2 - t} & \text{for } F=0 \ ; \\ \dfrac{a_{ij}^{eq}\cdot\lambda_{\rm LQ}^2}{M_{\rm LQ}^2 - u} & \text{for } |F|=2. \end{cases}$$

The same formulae apply also to the $q\bar{q}\to l^+l^-$ amplitude, with i and j labelling the chiralities of the initial quark and final lepton respectively.

Leptoquark states with $\beta = 1/2$ (coupling to both electron–quark and neutrino–quark pairs) contribute also to the charged current DIS at HERA $eq\to\nu q'$. For $M_{\rm LQ} \gg s^{1/2}$ the effective charged current contact-interaction coupling is given by

$$\eta^{\rm CC} \equiv \eta^{eu\nu d} = \left(a_{\rm LL}^{ed} - a_{\rm LL}^{eu}\right)\cdot\left(\frac{\lambda_{\rm LQ}}{M_{\rm LQ}}\right)^2. \qquad (4)$$

3 Experimental data

3.1 High-Q^2 DIS at HERA

Used in this analysis are the data from the years 1994–1997 on high-Q^2 e^+p NC DIS from both H1 [17] and ZEUS [18] as well as the recent results from e^-p NC DIS scattering [19,20]. The analysis takes into account expected and measured numbers of events in bins of Q^2. For simplicity let us consider a single Q^2 bin ranging from $Q^2_{\rm min}$ to $Q^2_{\rm max}$. Assume that $n_{\rm SM}$ events are expected from the standard model.

The leading-order doubly differential cross section for positron–proton NC DIS ($e^+p\to e^+X$) can be written as

$$\begin{aligned}\frac{{\rm d}^2\sigma^{\rm LO}}{{\rm d}x{\rm d}Q^2} = \frac{1}{16\pi}\sum_q & q(x,Q^2)\left\{|M_{\rm LR}^{eq}|^2 + |M_{\rm RL}^{eq}|^2\right. \\ & \left. + (1-y)^2\left[|M_{\rm LL}^{eq}|^2 + |M_{\rm RR}^{eq}|^2\right]\right\} \\ & + \bar{q}(x,Q^2)\left\{|M_{\rm LL}^{eq}|^2 + |M_{\rm RR}^{eq}|^2\right. \\ & \left. + (1-y)^2\left[|M_{\rm LR}^{eq}|^2 + |M_{\rm RL}^{eq}|^2\right]\right\},\end{aligned}$$

where x is the Bjorken variable, describing the fraction of the proton momentum carried by the struck quark (antiquark), $q(x,Q^2)$ and $\bar{q}(x,Q^2)$ are the quark and antiquark momentum distribution functions in the proton and M_{ij}^{eq} are the scattering amplitudes of (1), which can include contributions from leptoquark production or exchange processes.

The cross section integrated over the x and Q^2 range of an experimental Q^2 bin is

$$\sigma^{\rm LO}(\lambda_{\rm LQ}, M_{\rm LQ}) = \int\limits_{Q^2_{\rm min}}^{Q^2_{\rm max}} {\rm d}Q^2 \int\limits_{\frac{Q^2}{s\cdot y_{\rm max}}}^{1} {\rm d}x \frac{{\rm d}^2\sigma^{\rm LO}}{{\rm d}x{\rm d}Q^2}, \qquad (5)$$

where $y_{\rm max}$ is an upper limit on the reconstructed Bjorken variable y, $y = Q^2/(xs)$, imposed in the analysis. The number of events expected from the standard model with leptoquark contributions can now be calculated:

$$n(\lambda_{\rm LQ}, M_{\rm LQ}) = n_{\rm SM}\cdot\left(\frac{\sigma^{\rm LO}(\lambda_{\rm LQ}, M_{\rm LQ})}{\sigma^{\rm LO}_{\rm SM}}\right), \qquad (6)$$

where $\sigma^{\rm LO}_{\rm SM}$ is the standard model cross section calculated with formula (5) (setting $\lambda = 0$). Leading-order expectations of the leptoquark models are used to rescale the standard model prediction $n_{\rm SM}$ coming from detailed simulation of the experiment. This accounts for different experimental effects, and (to some extent) for higher-order QCD and electroweak corrections[3]. NLO QCD corrections to the resonant leptoquark production are introduced as an additional correction factor, based on [21].

For models with leptoquarks coupling to both electron-quark and neutrino–quark pairs ($S_0^{\rm L}$, S_1, $V_0^{\rm L}$ and V_1), HERA data on e^+p and e^-p CC DIS [17,19,22] are also included in the fit.

In the limit of heavy leptoquark masses ($M_{\rm LQ} \gg s^{1/2}$) the Q^2 distribution of NC and CC DIS events is most sensitive to the leptoquark couplings. For masses below $s^{1/2} \sim 300\,{\rm GeV}$, where direct leptoquark production becomes possible at HERA, better limits are obtained from studying the electron-jet invariant mass distribution. However, to correctly describe the narrow leptoquark resonance production and reconstruction, sizable QED and QCD corrections as well as complicated detector effects have to be taken into account. As these corrections could not be included in the analysis, the Q^2 distribution was used to constrain leptoquark couplings in the whole mass range. A comparison between limits calculated from the Q^2 distribution of the ZEUS e^+p NC DIS data [18] and the published ZEUS limits for $F=0$ leptoquarks [23][4] is presented in Fig. 2. Taking into account that the ZEUS analysis includes mass dependent selection cuts and that it was optimized for leptoquark search, the difference between the two approaches is surprisingly small. Direct ZEUS limits are at most 40% lower (depending on the model and the mass range) than the one obtained from the Q^2 distribution.

3.2 Measurements from LEP

Many measurements at LEP are sensitive to different kinds of "new physics". The leptoquark exchange contribution can directly be tested in the measurement of the total hadronic cross section above the Z^0 pole[5]. The leading-order formula for the total quark-pair production cross

[3] Correctly taken into account are only those corrections which are the same or similar for the standard model and for the cross section including leptoquark contributions

[4] Similar limits on the leptoquark couplings and masses have also been presented by the H1 Collaboration [24]

[5] For the leptoquark masses and couplings considered here the effects of the possible leptoquark exchange at $s^{1/2} = M_Z$ are completely negligible in comparison with the resonant Z^0 production

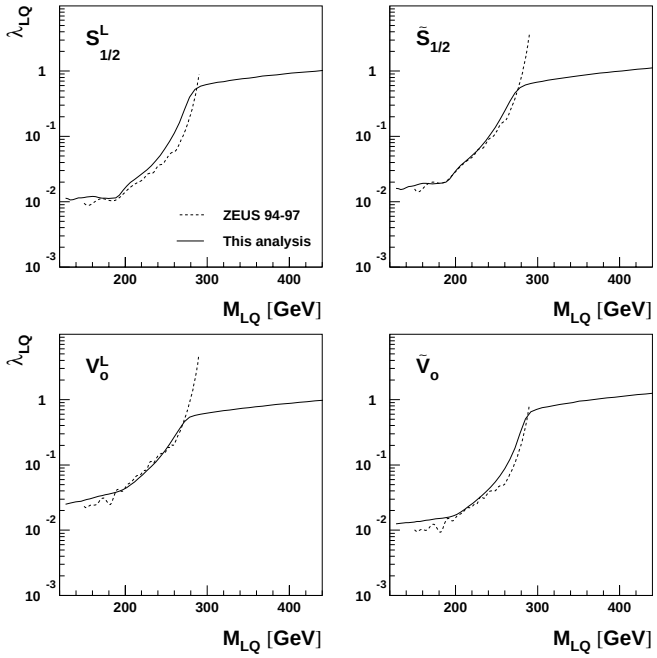

Fig. 2. Comparison between limits calculated from the Q^2 distribution of the ZEUS e^+p NC DIS data (this analysis) and the published ZEUS limits [23] for selected $F = 0$ leptoquarks, as indicated in the plot

section, $\sigma(e^+e^- \to q\bar{q})$, at an electron–positron center-of-mass energy squared s is

$$\sigma^{\rm LO}(s) = \frac{3s}{128\pi} \sum_q \int \mathrm{d}\cos\theta \times \left[\left(|M^{ee}_{\rm LL}|^2 + |M^{ee}_{\rm RR}|^2 \right) (1+\cos\theta)^2 + \left(|M^{ee}_{\rm LR}|^2 + |M^{ee}_{\rm RL}|^2 \right) (1-\cos\theta)^2 \right], \quad (7)$$

where M^{ee}_{ij} are the scattering amplitudes described by (3), including contributions from leptoquark exchange and θ is the quark production angle in the e^+e^- center-of-mass system. For comparison with measured experimental values, the expected standard model cross section $\sigma^{\rm SM}(s)$ quoted by experiments are rescaled using the ratio of the leading-order cross sections with and without leptoquark contribution:

$$\sigma(s, \lambda_{\rm LQ}, M_{\rm LQ}) = \sigma^{\rm SM}(s) \cdot \left(\frac{\sigma^{\rm LO}(s, \lambda_{\rm LQ}, M_{\rm LQ})}{\sigma^{\rm LO}_{\rm SM}} \right), \quad (8)$$

where $\sigma^{\rm LO}_{\rm SM}$ is the leading-order standard model cross section ($\lambda = 0$), calculated with (7). This takes into account possible experimental effects and higher-order QCD and electroweak corrections. Included in the analysis are data on $\sigma_{\rm had}$ from Aleph, Delphi, L3 and Opal experiments for center-of-mass energies up to 202 GeV [25–28]. All measurements are in good agreement with the standard model predictions. However, cross-section values obtained for $s^{1/2} = 192$–$202\,\mathrm{GeV}$ are on average about 2.5% above the predictions. The combined significance of this deviation is only about 2.3σ [29] but it has an important influence on the global analysis.

In the global analysis of electron–quark contact interactions [3], the strongest constraints on the contact-interaction couplings resulted from the LEP data on heavy quark production, R_q ($q = b, c$), and on forward–backward asymmetries, $A^q_{\rm FB}$. However, this is only the case for models assuming family universality. For the first-generation leptoquarks, the constraints resulting from LEP measurements based on heavy flavor tagging are much weaker than those resulting from hadronic cross-section measurements. Nevertheless, possible deviations in the $u\bar{u}$ and $d\bar{d}$ quark-pair production cross sections (resulting in the deviation of the total hadronic cross section) can also be constrained using results on R_c and R_b. Results on $A^q_{\rm FB}$ are included in the presented analysis for consistency with the previous study [3].

3.3 Drell–Yan lepton pair production at the Tevatron

Used in this analysis are data on Drell–Yan electron pair production ($p\bar{p} \to e^+e^-X$) from the CDF [30] and DØ [31] experiments. The leading-order cross section for lepton pair production in $p\bar{p}$ collisions is

$$\frac{\mathrm{d}^2\sigma^{\rm LO}}{\mathrm{d}M_{ll}\mathrm{d}Y} = \frac{M^3_{ll}}{192\pi s} \sum_q q(x_1)q(x_2) \int \mathrm{d}\cos\theta \times \left[\left(|M^{ee}_{\rm LL}|^2 + |M^{ee}_{\rm RR}|^2 \right) (1+\cos\theta)^2 + \left(|M^{ee}_{\rm LR}|^2 + |M^{ee}_{\rm RL}|^2 \right) (1-\cos\theta)^2 \right],$$

where M_{ll} is the invariant lepton pair mass, Y is the rapidity of the lepton pair, θ is the lepton production angle in their center-of-mass system, and x_1 and x_2 are the fractions of the proton and antiproton momenta carried by the annihilating $q\bar{q}$. When integrating over θ, the angular detector coverage is taken into account. The scattering amplitudes M^{ee}_{ij} and the parton density functions are calculated at a mass scale

$$\mu^2 = \hat{s} = x_1 x_2 s,$$

where s is the total proton–antiproton center-of-mass energy squared.

The cross section corresponding to the M_{ll} range from $M_{\rm min}$ to $M_{\rm max}$ is calculated as

$$\sigma^{\rm LO}(\lambda_{\rm LQ}, M_{\rm LQ}) = \int_{M_{\rm min}}^{M_{\rm max}} \mathrm{d}M_{ll} \int_{-Y_{\rm max}}^{Y_{\rm max}} \mathrm{d}Y \frac{\mathrm{d}^2\sigma}{\mathrm{d}M_{ll}\mathrm{d}Y}, \quad (9)$$

where $Y_{\rm max}$ is the upper limit on the rapidity of the produced lepton pair:

$$Y_{\rm max} = \ln \frac{\sqrt{s}}{M_{ll}}.$$

The cross section calculated with (9) is used to calculate the number of events expected from the standard model with leptoquark contribution using formula (6).

3.4 Direct limits from the Tevatron

The DØ and CDF experiments at the Tevatron presented limits on the first-generation scalar leptoquark masses from the search for leptoquark pair production in hard interactions ($p\bar{p} \to \mathrm{LQ}\overline{\mathrm{LQ}}X$). Both experiments see no leptoquark candidate events, with leptoquarks decaying into an electron and a jet, above a reconstructed leptoquark mass of 200 GeV [32,33]. The result of the NLO cross-section calculations[6] [34] can be parameterized in this mass region as

$$\sigma^S_{\mathrm{LQ}}(M_{\mathrm{LQ}}) \approx 114.6\,\mathrm{pb} \cdot \exp\left(-\frac{M_{\mathrm{LQ}}}{30.28\,\mathrm{GeV}}\right).$$

The expected number of leptoquark events reconstructed in the $eejj$ channel is

$$n_{\mathrm{exp}}(M_{\mathrm{LQ}}) = \epsilon\mathcal{L} \cdot \sigma^S_{\mathrm{LQ}}(M_{\mathrm{LQ}}) \sum_{\mathrm{LQ}} \beta^2_{\mathrm{LQ}},$$

where the sum is over leptoquark states within the considered multiplet and the combined effective luminosity (i.e. luminosity corrected for selection efficiency) for two experiments is $\epsilon\mathcal{L} \approx 78\,\mathrm{pb}^{-1}$. For leptoquark states with $\beta = 0.5$, the results of DØ search in $e\nu jj$ channel are also included in the analysis. Because of the assumed mass degeneration the mass limits for scalar leptoquark multiplets can be significantly higher than for single leptoquarks. For the $S^{\mathrm{R}}_{1/2}$ isospin doublet ($\sum \beta^2_{\mathrm{LQ}} = 2$) the combined limit is $M_{\mathrm{LQ}} > 263\,\mathrm{GeV}$, as compared with the published limit of 242 GeV for single leptoquark production [35].

For vector leptoquarks, the pair production cross section at the Tevatron strongly depends on the unknown (not constrained in the BRW model) anomalous leptoquark couplings. For the presented analysis the values giving the smallest vector leptoquark-pair production cross section were assumed [36]. The LO vector leptoquark production cross section has been parametrized as

$$\sigma^V_{\mathrm{LQ}}(M_{\mathrm{LQ}}) \approx 268.1\,\mathrm{pb} \cdot \exp\left(-\frac{M_{\mathrm{LQ}}}{28.65\,\mathrm{GeV}}\right).$$

Only the DØ experiment has presented limits on the vector leptoquark masses in the minimum cross-section model [37]. The limit $M_{\mathrm{LQ}} > 245\,\mathrm{GeV}$ (for $\beta = 1$) corresponds to the effective luminosity of $\epsilon\mathcal{L} \approx 58\,\mathrm{pb}^{-1}$.

3.5 Data from low energy experiments

The low energy data are included in the present analysis in exactly the same way as in the contact-interaction analysis [3]. For all leptoquark models the following constraints from low energy experiments are considered.

(1) Atomic parity violation (APV): The standard model predicts parity non-conservation in atoms caused (in lowest order) by the Z^0 exchange between electrons and quarks in the nucleus. Experimental results on parity violation in atoms are given in terms of the weak charge Q_W of the nuclei. The standard model prediction for Q_W is based on the very precise measurement of the $\sin^2\Theta_{\mathrm{W}}$ at LEP1 and SLD. A new determination of Q_W for cesium atoms was recently reported [9]. The experimental result differs from the standard model prediction by

$$\Delta Q^{\mathrm{Cs}}_W \equiv Q^{\mathrm{meas}}_W - Q^{\mathrm{SM}}_W = 1.13 \pm 0.46.$$

As already mentioned in the Introduction, this 2.5σ discrepancy between the measurement and standard model predictions induces significant evidence for some leptoquark models. Also other "new physics" processes, as for example $Z^{0\prime}$ exchange, were proposed as a possible explanation for the APV measurement. One has to take into account that these new processes can also affect precision measurements at LEP1 and the determination of $\sin^2\Theta_{\mathrm{W}}$, making the analysis much more difficult. However, for the leptoquark masses and couplings considered here the effects of the possible leptoquark exchange at $s^{1/2} = M_Z$ can be safely neglected.

The leptoquark contribution to Q_W is

$$\begin{aligned}\Delta Q_W = &\frac{2Z+N}{\sqrt{2}G_{\mathrm{F}}}\left(\eta^{eu}_{\mathrm{LL}} + \eta^{eu}_{\mathrm{LR}} - \eta^{eu}_{\mathrm{RL}} - \eta^{eu}_{\mathrm{RR}}\right)\\ &+ \frac{Z+2N}{\sqrt{2}G_{\mathrm{F}}}\left(\eta^{ed}_{\mathrm{LL}} + \eta^{ed}_{\mathrm{LR}} - \eta^{ed}_{\mathrm{RL}} - \eta^{ed}_{\mathrm{RR}}\right),\end{aligned}$$

where η^{eq}_{ij} are the effective couplings given by (2).

(2) Electron–nucleus scattering: The limits on possible leptoquark contributions to electron–nucleus scattering at low energies can be extracted from the polarization asymmetry measurement

$$A = \frac{\mathrm{d}\sigma_{\mathrm{R}} - \mathrm{d}\sigma_{\mathrm{L}}}{\mathrm{d}\sigma_{\mathrm{R}} + \mathrm{d}\sigma_{\mathrm{L}}},$$

where $\mathrm{d}\sigma_{\mathrm{L(R)}}$ denotes the differential cross section of left- (right-) handed electron scattering. The polarization asymmetry directly measures the parity violation resulting from the interference between Z^0 and γ scattering amplitudes. For isoscalar targets, taking into account valence quark contributions only, the polarization asymmetry for elastic electron scattering is

$$A = -\frac{3\sqrt{2}G_{\mathrm{F}}Q^2}{20\pi\alpha_{\mathrm{em}}}\left[2\left(g^u_{\mathrm{L}} + g^u_{\mathrm{R}}\right) - \left(g^d_{\mathrm{L}} + g^d_{\mathrm{R}}\right)\right],$$

where Q^2 is the four-momentum transfer and the effective electroweak coupling of the quark is modified by the leptoquark contribution

$$g^q_i|_{\mathrm{eff}} = g^q_i - \frac{\eta^{eq}_{\mathrm{L}i}}{2\sqrt{2}G_{\mathrm{F}}}. \tag{10}$$

The data used in this analysis come from the SLAC eD experiment [38], the Bates eC experiment [39] and the Mainz experiment on eBe scattering [40].

For leptoquarks contributing to charged current processes, additional constraints come from the following.

[6] Assuming a mass scale $\mu = 2M_{\mathrm{LQ}}$

(1) Lepton–hadron universality of weak charged currents. New charged current interactions would affect the measurement of V_{ud} element of the Cabibbo–Kobayashi–Maskawa (CKM) matrix, leading to an effective violation of unitarity [41,42]. The new experimental constraint is [43]

$$|V_{ud}|^2 + |V_{us}|^2 + |V_{ub}|^2 = 0.9959 \pm 0.0019,$$

whereas the expected leptoquark contribution is

$$V_{ud} = V_{ud}^{\rm SM} \cdot \left(1 - \frac{\eta^{\rm CC}}{2\sqrt{2}G_{\rm F}}\right),$$

with $\eta^{\rm CC}$ given by (4).

(2) Electron-muon universality. In a similar way new charged current interactions would also lead to effective violation of e–μ universality in charged pion decay [41]. The current experimental value of $R = \Gamma(\pi^- \to e\bar{\nu})/\Gamma(\pi^- \to \mu\bar{\nu})$ is [44]

$$\frac{R_{\rm meas}}{R_{\rm SM}} = 0.9966 \pm 0.030,$$

whereas the expected contribution from leptoquark exchange is

$$\mathrm{R}|_{\rm meas} = R_{\rm SM} \cdot \left(1 - \frac{\eta^{\rm CC}}{2\sqrt{2}G_{\rm F}}\right)^2.$$

It is important to notice that data in the charged current sector also indicate a possible deviation from the standard model predictions: a slight violation of the unitarity of the CKM matrix and of the e-μ universality. The combined significance of these two results is about 2.4σ and has a considerable influence on the presented analysis.

4 Analysis method

The analysis method is similar to the one used in a recently published analysis [3]. For every leptoquark coupling and mass value the probability function describing the agreement between the model and the data is calculated:

$$\mathcal{P}(\lambda_{\rm LQ}, M_{\rm LQ}) \sim \prod_i P_i(\lambda_{\rm LQ}, M_{\rm LQ}). \tag{11}$$

The product runs over all experimental data i. The logarithm of the probability function $\ln \mathcal{P}$ is the so-called log-likelihood function, which is often used in similar analyses:

$$\ln \mathcal{P}(\lambda_{\rm LQ}, M_{\rm LQ}) = \sum_i \ln P_i(\lambda_{\rm LQ}, M_{\rm LQ}).$$

The data used in this analysis can be divided into two classes.

(1) For experiments in which a result is presented as a single number with an error which is considered to reflect a Gaussian probability distribution, the probability function can be written as

$$P_i(\lambda_{\rm LQ}, M_{\rm LQ}) \sim \exp\left(-\frac{1}{2}\frac{(F(\lambda_{\rm LQ}, M_{\rm LQ}) - \Delta A)^2}{\sigma_A^2}\right), \tag{12}$$

where ΔA is the difference between the measured value and the standard model prediction, σ_A is the measurement error and $F(\lambda_{\rm LQ}, M_{\rm LQ})$ is the expected leptoquark contribution to the measured value. This approach is used for all low energy data as well as for the LEP hadronic cross-section measurements.

(2) On the other hand, if the experimentally measured quantity is the number of events of a particular kind (e.g. HERA high-Q^2 data or Drell–Yan lepton pairs and direct search results from the Tevatron), and especially when this number is small, the probability is better described by the Poisson distribution

$$P_i(\lambda_{\rm LQ}, M_{\rm LQ}) \sim \frac{n(\lambda_{\rm LQ}, M_{\rm LQ})^N \cdot \exp(-n(\lambda_{\rm LQ}, M_{\rm LQ}))}{N!}, \tag{13}$$

where N and $n(\lambda_{\rm LQ}, M_{\rm LQ})$ are the measured and expected numbers of events in a given experiment, respectively, and $n(\lambda_{\rm LQ}, M_{\rm LQ})$ takes into account a possible leptoquark contribution. This approach has been used for the HERA and the Tevatron data.

For low energy data the total measurement error can be used in (12) taking into account both statistical and systematic errors. For collider data, formula (12) or (13) is used to take into account the statistical error of the measurement only. The systematic errors are assumed to be correlated to 100% within a given data set (e.g. e^+p NC DIS data from ZEUS). This approach as well as the migration corrections used for HERA and Tevatron Drell–Yan results are discussed in detail in [3].

The probability function $\mathcal{P}(\lambda_{\rm LQ}, M_{\rm LQ})$ summarizes our current experimental knowledge about possible leptoquark couplings and masses. As $\mathcal{P}$ is not a probability distribution, it does not satisfy any normalization condition. Instead it is convenient to rescale the probability function in such a way that for the standard model it has the value of 1:

$$\begin{aligned} \mathcal{P}(\lambda_{\rm LQ} = 0, M_{\rm LQ}) &= 1, \\ \text{or} \quad \ln \mathcal{P}(\lambda_{\rm LQ} = 0, M_{\rm LQ}) &= 0. \end{aligned} \tag{14}$$

Using the probability function $\mathcal{P}(\lambda_{\rm LQ}, M_{\rm LQ})$ two types of limits in $(\lambda_{\rm LQ}, M_{\rm LQ})$ space are calculated:

(1) Rejected are all models (parameter values) which result in

$$\begin{aligned} \mathcal{P}(\lambda_{\rm LQ}, M_{\rm LQ}) &< 0.05, \\ \text{or} \quad \ln \mathcal{P}(\lambda_{\rm LQ}, M_{\rm LQ}) &< -3.0. \end{aligned}$$

This is taken as the definition of the 95% confidence level (CL) exclusion limit. Exclusion limits presented in this

paper are lower limits in case of leptoquark mass $M_{\rm LQ}$ and upper limits in case of $\lambda_{\rm LQ}$ or $\lambda_{\rm LQ}/M_{\rm LQ}$.

(2) Some leptoquark models turn out to describe the data much better than the standard model:

$$\mathcal{P}_{\rm max} \equiv \max_{\lambda_{\rm LQ}, M_{\rm LQ}} \mathcal{P}(\lambda_{\rm LQ}, M_{\rm LQ}) \gg 1.$$

In that case the 95% CL *signal limit* corresponding to the uncertainty on the "best" values of $\lambda_{\rm LQ}$ and $M_{\rm LQ}$ is defined by the condition

$$\mathcal{P}(\lambda_{\rm LQ}, M_{\rm LQ}) > 0.05 \cdot \mathcal{P}_{\rm max}$$
$$\text{or} \quad \ln \mathcal{P}(\lambda_{\rm LQ}, M_{\rm LQ}) < \ln \mathcal{P}_{\rm max} - 3.0$$

In the previous analysis [3] no significant deviations from the standard model were observed. In such a case both definitions give similar results and there is no need to distinguish between exclusion and signal limits.

5 Results

In the limit of very high leptoquark masses (contact-interaction approximation) the probability function depends only on the $\lambda_{\rm LQ}/M_{\rm LQ}$ ratio. Using the global model probability $\mathcal{P}(\lambda_{\rm LQ}, M_{\rm LQ})$, as defined by (11), the value $(\lambda_{\rm LQ}/M_{\rm LQ})_{\rm max}$ giving the maximum probability is determined for each model. The results are presented in Table 3. The attributed errors, quoted for models which give better description of the data than the standard model (i.e. $(\lambda_{\rm LQ}/M_{\rm LQ})_{\rm max} > 0$) correspond to the decrease in $\ln \mathcal{P}(\lambda_{\rm LQ}, M_{\rm LQ})$ by 1/2. The probability functions $\mathcal{P}(\lambda_{\rm LQ}, M_{\rm LQ})$ for different leptoquark models are shown in Fig. 3.

For 8 out of 14 leptoquark models, the standard model gives the best description of the considered experimental data ($(\lambda_{\rm LQ}/M_{\rm LQ})_{\rm max} = 0$). 95% CL exclusion limits for $\lambda_{\rm LQ}/M_{\rm LQ}$ range for these models from $0.12\,{\rm TeV}^{-1}$ (for the $V_0^{\rm L}$ model) to $0.29\,{\rm TeV}^{-1}$ (for the $S_{1/2}^{\rm L}$ model). The other 6 models are able to describe the data better than the standard model. In all cases the "best" coupling to mass ratio turns out to be of the order of $0.3\,{\rm TeV}^{-1}$.

The best description of the data is given by the S_1 model for $(\lambda_{\rm LQ}/M_{\rm LQ})_{\rm max} = 0.28 \pm 0.04\,{\rm TeV}^{-1}$ resulting in the maximum probability $\mathcal{P}_{\rm max} = 367$ ($\ln \mathcal{P}_{\rm max} = 5.9$). For the Gaussian probability function this would correspond to about 3.4σ deviation from the standard model. The effect is mainly due to the APV result: the contribution of the APV measurement to the maximum probability is $P = 20$ ($\ln P = 3.0$), corresponding to a 2.4σ deviation from the standard model. The result is also supported by the low energy charged current data (unitarity of the CKM matrix and e-μ universality; $\ln P = 2.4$, 2.2σ effect) and LEP2 hadronic cross-section measurements ($\ln P = 0.5$, 1.0σ effect). Contributions of different data sets to the S_1 model probability function are presented in Fig. 4. The fitted value of $(\lambda_{\rm LQ}/M_{\rm LQ})_{\rm max}$ results in almost the best description of both APV and low energy charged current data, whereas LEP2 hadronic cross-section measurements suggest even higher values of

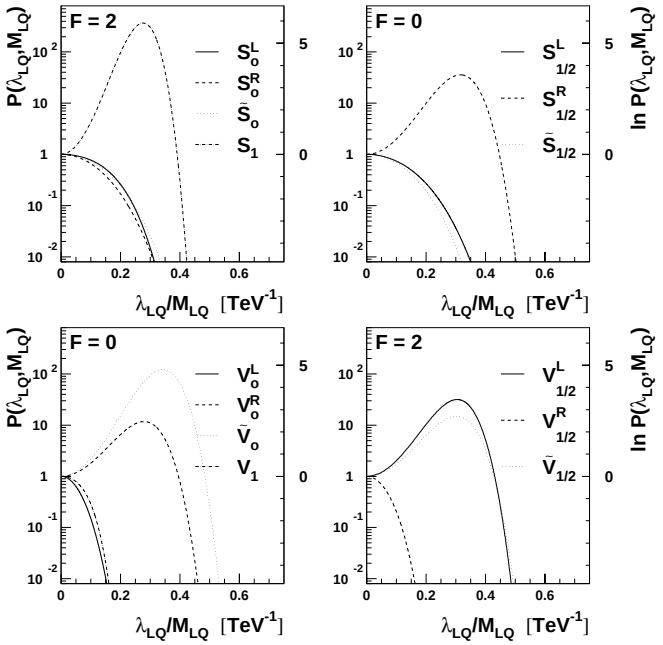

Fig. 3. Probability function $\mathcal{P}(\lambda_{\rm LQ}, M_{\rm LQ})$ (left-hand scale) and the log-likelihood function $\ln \mathcal{P}(\lambda_{\rm LQ}, M_{\rm LQ})$ (right-hand scale), in the limit of very high leptoquark masses, for different leptoquark models as indicated on the plot

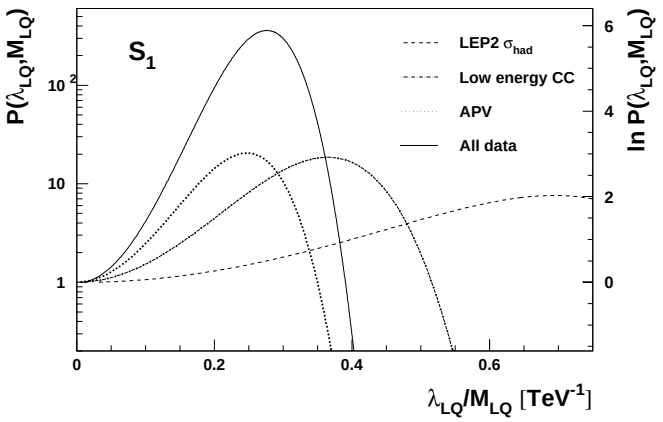

Fig. 4. Contributions of different data sets (as indicated on the plot) to the global probability functions $\mathcal{P}(\lambda_{\rm LQ}, M_{\rm LQ})$ (left-hand scale) and to the log-likelihood function $\ln \mathcal{P}(\lambda_{\rm LQ}, M_{\rm LQ})$ (right-hand scale), for the S_1 model in the limit of very high leptoquark masses

$\lambda_{\rm LQ}/M_{\rm LQ} \sim 0.7\,{\rm TeV}^{-1}$. The 95% CL signal limit, corresponding to a model with the probabilities $\mathcal{P} > 0.05 \cdot \mathcal{P}_{\rm max}$, is $0.15 < \lambda_{\rm LQ}/M_{\rm LQ} < 0.36\,{\rm TeV}^{-1}$.

The $\tilde{V}_0$ model also gives a very good description of the data, resulting in $\mathcal{P}_{\rm max} = 122$ ($\ln P = 4.8$ corresponding to about 3.1σ). In this case the APV result ($\ln P = 3.1$, 2.5σ) is strongly supported by the LEP2 data ($\ln P = 1.3$, 1.6σ). The $S_{1/2}^{\rm R}$ and $V_{1/2}^{\rm L}$ models describe the APV measurement as well but they do not improve the description of other data. For $V_0^{\rm R}$ and $\tilde{V}_{1/2}$ models, the coupling values required to explain APV data are disfavored by other experiments (mainly by LEP2 hadronic cross-section mea-

Table 3. Coupling to mass ratio, $(\lambda_{\rm LQ}/M_{\rm LQ})_{\rm max}$, resulting in the best description of the experimental data in the contact-interaction approximation, and the corresponding model probability $\mathcal{P}_{\rm max}$ and the log-likelihood $\ln\mathcal{P}_{\rm max}$, for different leptoquark models, as indicated in the table. The errors attributed to non-zero $\lambda_{\rm LQ}/M_{\rm LQ}$ values correspond to the decrease of $\ln\mathcal{P}$ by 1/2. Also given are 95% CL signal (for models with $\mathcal{P}_{\rm max} > 20$) and (upper) exclusion limits on $\lambda_{\rm LQ}/M_{\rm LQ}$, and (lower) exclusion limits on leptoquark masses $M_{\rm LQ}$

	Best description			95% CL signal	95% CL exclusion limits	
Model	$(\lambda_{\rm LQ}/M_{\rm LQ})_{\rm max}$ [TeV^{-1}]	$\mathcal{P}_{\rm max}$	$\ln\mathcal{P}_{\rm max}$	$(\lambda_{\rm LQ}/M_{\rm LQ})$ [TeV^{-1}]	$(\lambda_{\rm LQ}/M_{\rm LQ})$ [TeV^{-1}]	$M_{\rm LQ}$ [GeV]
$S_0^{\rm L}$	0	1.0	0.0		0.27	213
$S_0^{\rm R}$	0	1.0	0.0		0.25	242
$\tilde{S}_0$	0	1.0	0.0		0.28	242
$S_{1/2}^{\rm L}$	0	1.0	0.0		0.29	229
$S_{1/2}^{\rm R}$	0.32 ± 0.06	35.8	3.6	0.09–0.44	0.49	245
$\tilde{S}_{1/2}$	0	1.0	0.0		0.26	233
S_1	0.28 ± 0.04	367.	5.9	0.15–0.36	0.41	245
$V_0^{\rm L}$	0	1.0	0.0		0.12	230
$V_0^{\rm R}$	0.28 ± 0.07	11.7	2.5		0.44	231
$\tilde{V}_0$	0.34 ± 0.06	122.	4.8	0.16–0.46	0.52	235
$V_{1/2}^{\rm L}$	0.30 ± 0.06	31.7	3.5	0.08–0.42	0.47	235
$V_{1/2}^{\rm R}$	0	1.0	0.0		0.13	262
$\tilde{V}_{1/2}$	0.30 ± 0.07	14.8	2.7		0.47	244
V_1	0	1.0	0.0		0.14	254

surements) resulting in even smaller $\mathcal{P}_{\rm max}$ values. Signal limits for 4 models which result in $\mathcal{P}_{\rm max} > 20$ are included in Table 3. For models with $\mathcal{P}_{\rm max} > 1$ (models describing the APV data) the 95% CL exclusion limits on $\lambda_{\rm LQ}/M_{\rm LQ}$ range from $0.41\,{\rm TeV}^{-1}$ (for the S_1 model) to $0.52\,{\rm TeV}^{-1}$ (for the $\tilde{V}_0$ model).

All of the results presented above were based on the contact-interaction approximation, which is valid for leptoquark masses above about 1 TeV. In the second part of the analysis presented lower leptoquark masses were also considered. In that case, leptoquark constraints have to be studied in terms of the leptoquark coupling and the leptoquark mass as two independent parameters.

Below 1 TeV, effects of the finite leptoquark mass reduce the virtual leptoquark exchange contribution to the expected LEP and Tevatron cross sections. However, this effect is small and the asymptotic limit on $\lambda_{\rm LQ}/M_{\rm LQ}$ increases by only about 10% for leptoquark masses $M_{\rm LQ} \sim 300\,{\rm GeV}$. For masses below 300 GeV, the limits on $\lambda_{\rm LQ}$ become much stronger because of the direct searches at HERA and at the Tevatron. Combined constraints on the leptoquark coupling and mass are derived from the probability function $\mathcal{P}(\lambda_{\rm LQ}, M_{\rm LQ})$, as described in Sect. 4. The 95% CL exclusion limits in $(\lambda_{\rm LQ}, M_{\rm LQ})$ space, for different models of scalar and vector leptoquarks are presented in Fig. 5. The 95% CL exclusion limits on the leptoquark masses (i.e. largest mass values resulting in $\mathcal{P} \leq 0.05$ for any value of $\lambda_{\rm LQ}$) are included in Table 3.

The parameter values resulting in the best description of the experimental data were also searched for finite leptoquark masses, varying $\lambda_{\rm LQ}$ and $M_{\rm LQ}$ independently. Only for one leptoquark model an improvement has been obtained as compared with the asymptotic solution. For $M_{\rm LQ} = 276\,{\rm GeV}$ and $\lambda_{\rm LQ} = 0.095$ the maximum probability $\mathcal{P}_{\rm max} = 142$ ($\ln\mathcal{P} = 5.0$) is obtained for the $\tilde{V}_0$ model. This corresponds to about 3.1σ deviation from the standard model. The effect is mainly due to the new APV measurement ($\ln P = 3.0$, 2.4σ effect), but is also supported by the excess of high-Q^2 NC e^+p DIS events at HERA ($\ln P = 1.4$, 1.7σ effect) and the LEP2 hadronic cross-section measurements ($\ln P = 1.2$, 1.5σ effect). For all HERA, LEP and low energy data the maximum probability turns out to be $\mathcal{P}_{\rm max} = 367$ (as compared to $\mathcal{P}_{\rm max} = 122$ in the contact-interaction limit). However, the value of $\tilde{V}_0$ leptoquark mass of $M_{\rm LQ} = 276\,{\rm GeV}$ is already strongly disfavored by the negative direct search results from the Tevatron ($P = 0.36$, $\ln P = -1.0$). Contributions of different data sets to the probability function for the $\tilde{V}_0$ model with $M_{\rm LQ} = 276$ GeV are presented in Fig. 6. A very good description of APV and HERA high-Q^2 data is obtained for the fitted value of $\lambda_{\rm LQ}$, whereas LEP2 measurements again suggest higher values of $\lambda_{\rm LQ} \sim 0.16$. The ratio of the predicted e^+p cross section at high Q^2 to the standard model cross section is shown in Fig. 7 together with the corresponding H1 [17] and ZEUS [18] data. The hypothesis of the $\tilde{V}_0$ leptoquark production can describe the excess of events at highest

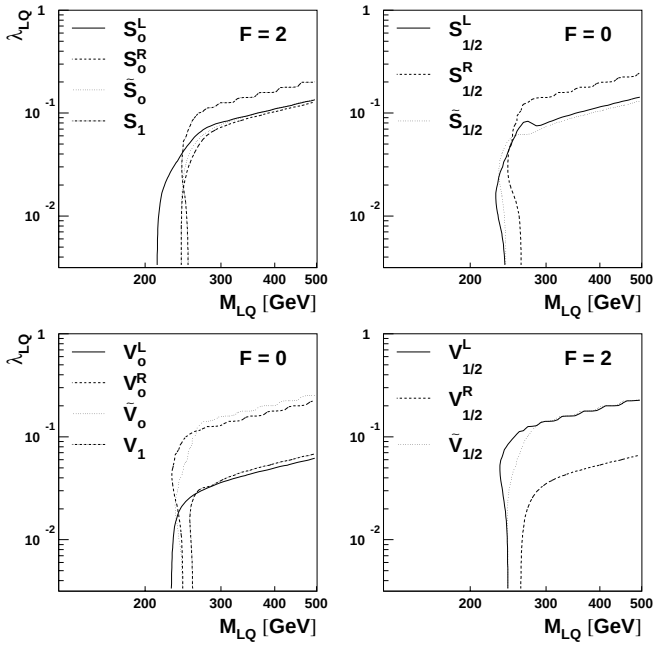

Fig. 5. 95% CL exclusion limits in $(\lambda_{\rm LQ}, M_{\rm LQ})$ space, for different leptoquark models, as indicated in the plot. Excluded are coupling and mass values above or to the left of the limit curves

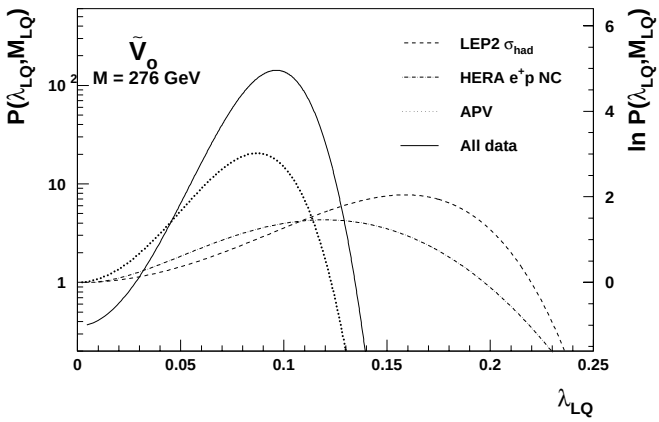

Fig. 6. Contributions of different data sets (as indicated on the plot) to the global probability functions $\mathcal{P}(\lambda_{\rm LQ}, M_{\rm LQ})$ (left-hand scale) and to the log-likelihood function $\ln \mathcal{P}(\lambda_{\rm LQ}, M_{\rm LQ})$ (right-hand scale), for the $\tilde{V}_0$ model with $M_{\rm LQ} = 276\,\mathrm{GeV}$

Q^2 not affecting the perfect agreement with the standard model at $Q^2 < 10000\,\mathrm{GeV}^2$. Also shown in Fig. 7 is the predicted deviation of the total hadronic cross section at LEP as a function of $s^{1/2}$. A best fit of the $\tilde{V}_0$ model results in the cross-section increase at highest $s^{1/2}$ by about 1%, which is consistent with the available data. From the fit of a two-dimensional Gaussian distribution in the close neighborhood of the maximum of the probability function $\mathcal{P}(\lambda_{\rm LQ}, M_{\rm LQ})$, the errors on the $\tilde{V}_0$ parameter values were estimated:

$$M_{\rm LQ} = 276 \pm 7\,\mathrm{GeV},$$
$$\lambda_{\rm LQ} = 0.095 \pm 0.015.$$

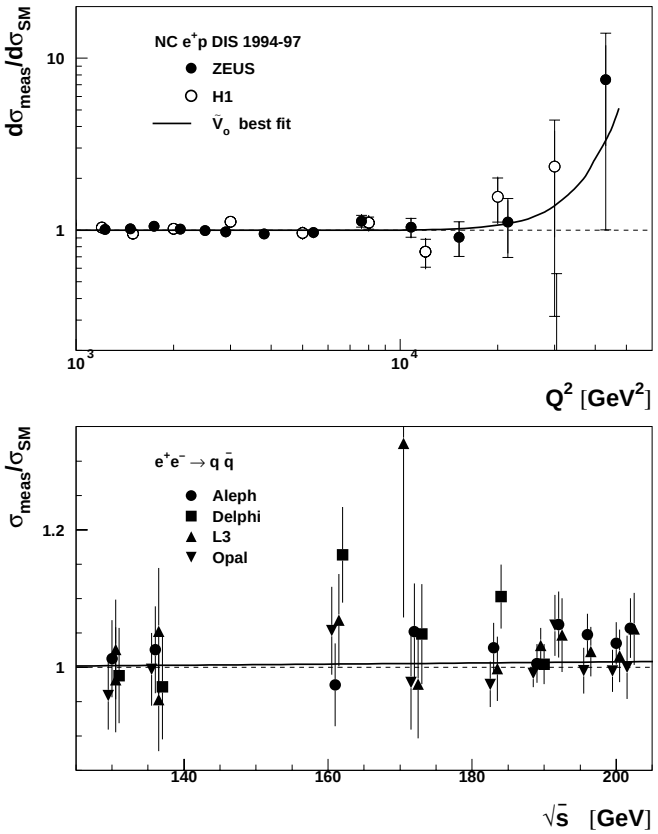

Fig. 7. Cross-section deviations from the standard model resulting from the fit of the $\tilde{V}_0$ model (thick solid line) compared with HERA NC e^+p DIS cross-section results (upper plot) and LEP2 hadronic cross-section results (lower plot)

The local maximum of the probability function at $M_{\rm LQ} = 274\,\mathrm{GeV}$ is also observed for the $S^{\rm R}_{1/2}$ model ($\mathcal{P} = 20.3$, as compared with $\mathcal{P}_{\rm max} = 35.8$ obtained in the high leptoquark mass limit). This maximum is due to APV and HERA data, but is strongly suppressed by the Tevatron direct search results[7]. Signal limits in the $(\lambda_{\rm LQ}, M_{\rm LQ})$ space were studied for all leptoquark models which resulted in the description of the experimental data which was much better than the standard model ($\mathcal{P}_{\rm max} > 20$). Best parameter values and estimated 95% CL lower limits on the leptoquark masses are summarized in Table 4. In Fig. 8, the signal limits at 68% and 95% CL are compared with exclusion limits in the $(\lambda_{\rm LQ}, M_{\rm LQ})$ space.

The presented evidence for the possible existence of the leptoquark type objects results predominantly from the new data on the parity violation in cesium atoms [9]. The value of the cesium weak charge obtained from this measurement is about 2.5σ away from the standard model predictions. However, the evaluation of the weak charge of the nucleus strongly depends on the theoretical calculations of the cesium atomic structure. The reliability of the theoretical calculations used in [9] has been questioned

[7] For the $S^{\rm R}_{1/2}$ isospin doublet the combined Tevatron 95% CL limit is $M_{\rm LQ} > 263\,\mathrm{GeV}$, as compared with the published limit of 242 GeV for single leptoquark production (see Sect. 3.4)

Table 4. Coupling $\lambda_{\rm LQ}|_{\rm max}$ and mass $M_{\rm LQ}|_{\rm max}$ values resulting in the best description of the experimental data and the corresponding model probability $\mathcal{P}_{\rm max}$ for different leptoquark models, as indicated in the table. Also given are 95% CL lower limits on the leptoquark mass (signal limits). Shown in the table are only those models which give a much better description of the experimental data than the standard model ($\mathcal{P}_{\rm max} > 20$). When the best description is obtained in the very high mass limit, $(\lambda_{\rm LQ}/M_{\rm LQ})_{\rm max}$ is given

Model	$\mathcal{P}_{\rm max}$	$\ln \mathcal{P}_{\rm max}$	$\lambda_{\rm LQ}\|_{\rm max}$	$M_{\rm LQ}\|_{\rm max}$ [GeV]	$(\lambda_{\rm LQ}/M_{\rm LQ})_{\rm max}$ [TeV^{-1}]	95% CL limit on $M_{\rm LQ}$ [GeV]
$S^{\rm R}_{1/2}$	35.8	3.6			0.32 ± 0.06	258
S_1	367.	5.9			0.28 ± 0.04	267
$\tilde{V}_0$	142.	5.0	0.095 ± 0.015	276 ± 7		259
$V^{\rm L}_{1/2}$	31.7	3.5			0.30 ± 0.06	254

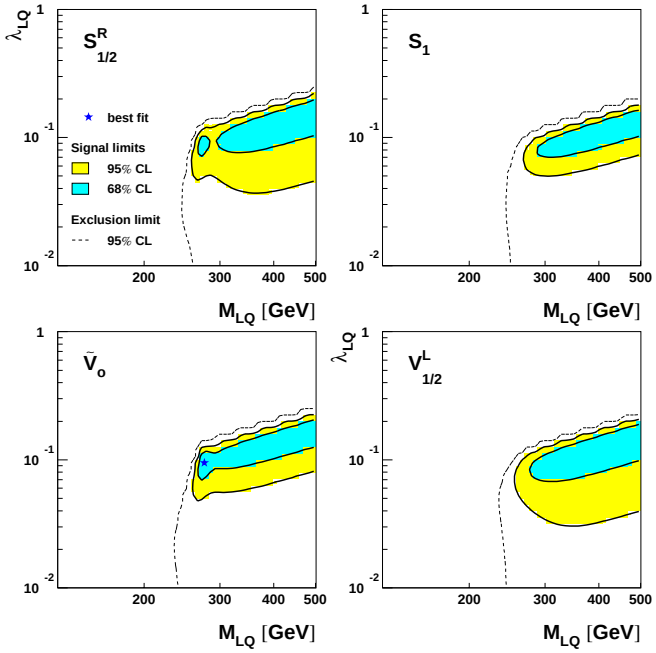

Fig. 8. Signal limits on 68% and 95% CL for different leptoquark models, as indicated in the plot. Dashed lines indicate the 95% CL exclusion limits. For the $\tilde{V}_0$ model a star indicates the best fit parameters. For other models the best fit is obtained in the contact-interaction limit $M_{\rm LQ} \to \infty$

in a recent paper [45]. The author claims that an important contribution from the so-called Breit interactions was not correctly taken into account. The analysis presented in [45], based on the third-order calculations, resulted in a 0.9% correction to the cesium weak charge. As a result, the previously observed deviation from the standard model predictions is reduced to the 1.2σ level.

When the value of the cesium weak charge reported in [45] is used in the global analysis results change drastically. Some leptoquark models still describe the existing experimental data slightly better than the standard model, but in most cases the effect is below 2σ. This is because constraints resulting from the corrected value of the cesium weak charge suppress the possible effects indicated by other experiments. The highest maximum probability $\mathcal{P}_{\rm max} = 14.5$ is observed for the S_1 leptoquark model with $(\lambda_{\rm LQ}/M_{\rm LQ})_{\rm max} = 0.23 \pm 0.05\,{\rm TeV}^{-1}$, corresponding to 2.3σ deviation from the standard model.

On the other hand, if an average value of the cesium weak charge from [9] and [45] is used, and the difference between the two theoretical calculations is taken as a conservative estimate of the theoretical uncertainty, the influence of the APV measurement on the global analysis is reduced. The best description of all data is again given by the S_1 model with $(\lambda_{\rm LQ}/M_{\rm LQ})_{\rm max} = 0.28 \pm 0.05\,{\rm TeV}^{-1}$. The maximum probability $\mathcal{P}_{\rm max} = 33.5$ corresponds to a 2.7σ effect. Also the $\tilde{V}_0$ model gives a sizable improvement in the description of the data, resulting in $\mathcal{P}_{\rm max} = 13.0$ (2.3σ effect) for $M_{\rm LQ} = 276 \pm 7\,{\rm GeV}$ and $\lambda_{\rm LQ} = 0.094 \pm 0.020$.

Results of the global analysis turn out to be very sensitive to both the outcome of the theoretical calculations of the cesium atomic structure and to their estimated uncertainty. Existing discrepancies between different theoretical calculations have to be clarified before any definite statement can be made on the possible signal for "new physics".

6 Summary

Data from HERA, LEP and the Tevatron as well as from low energy experiments were used to constrain the Yukawa couplings for scalar and vector leptoquarks in the Buchmüller–Rückl–Wyler effective model. In the limit of very high leptoquark masses, constraints on the coupling to mass ratio were studied using the contact-interaction approximation. Some leptoquark models are found to describe the existing experimental data much better than the standard model. The best description of the data is obtained for the S_1 model with $M_{\rm LQ} \gg 300\,{\rm GeV}$ and $\lambda_{\rm LQ}/M_{\rm LQ} = 0.28 \pm 0.04\,{\rm TeV}^{-1}$ and for the $\tilde{V}_0$ model with $M_{\rm LQ} = 276 \pm 7\,{\rm GeV}$ and $\lambda_{\rm LQ} = 0.095 \pm 0.015$. In both cases the increase of the global probability corresponds to more than 3σ deviation from the standard model. The effect is mainly due to the new data on atomic parity violation in cesium, but is also supported by LEP2 hadronic cross-section results and HERA NC e^+p DIS (for the $\tilde{V}_0$ model) or low energy CC data (for the S_1 model). Other

data considered in this analysis are also in good agreement with predictions of these models. If the observed $\tilde{V}_0$ signal is real it could become visible in the new HERA e^+p data, which are now being collected at increased center-of-mass energy[8].

The results presented strongly depend on the validity of the theoretical calculations used in the extraction of the cesium weak charge from the experimental data. The precision of these calculations has to be verified.

Acknowledgements. I would like to thank all members of the Warsaw HEP group and of the ZEUS Collaboration for support, encouragement, many useful comments and suggestions. Special thanks are due to K. Doroba, J. Kalinowski and U. Katz for many valuable comments to this paper. This work has been partially supported by the Polish State Committee for Scientific Research (grant No. 2 P03B 035 17).

References

1. The H1 Collaboration, C. Adloff et al., Z. Phys. C **74**, 191 (1997)
2. The ZEUS Collaboration, J. Breitweg et al., Z. Phys. C **74**, 207 (1997)
3. A.F. Żarnecki, Eur. Phys. J. C **11**, 539 (1999)
4. A.F. Żarnecki, hep-ph/0006196
5. R. Rückl, Phys. Lett. B **129**, 363 (1983); E. Eichten, K. Lane, M. Peskin, Phys. Rev. Lett. **50**, 811 (1983)
6. P. Haberl, F. Schrempp, H.-U. Martyn, Proceedings Workshop Physics at HERA, edited by W. Buchmüller, G. Ingelman (Hamburg 1991), vol. 2, p. 1133
7. The ZEUS Collaboration, J. Breitweg et al., Eur. Phys. J C **14**, 239 (2000)
8. C.S. Wood et al., Science **275**, 1759 (1997); S.A. Blundell, J. Sapirstein, W.R. Johnson, Phys. Rev D **45**, 1602 (1992)
9. S.C. Bennett, C.E. Wieman, Phys. Rev. Lett. **82**, 2484 (1999)
10. W. Buchmüller, R. Rückl, D. Wyler, Phys. Lett. B **191**, 442 (1987); Erratum: B **448**, 320 (1999)
11. J. Kalinowski, R. Rückl, H. Spiesberger, P.M. Zerwas, Z. Phys. C **74**, 595 (1997)
12. V. Barger, K. Cheung, K. Hagiwara, D. Zeppenfeld, Phys. Rev. D **57**, 391 (1998); D. Zeppenfeld, K. Cheung, MADPH-98-1081, hep-ph/9810277
13. Gi-Chol Cho, K. Hagiwara, S. Matsumoto, Eur. Phys. J. C **5**, 155 (1998)
14. V. Barger, K. Cheung, hep-ph/0002259
15. J.C. Pati, A. Salam, Phys. Rev. D **10**, 275 (1974); H. Georgi, S.L. Glashow, Phys. Rev. Lett. **32**, 438 (1974); J.L. Hawett, T.G. Rizzo, Phys. Rep. **183**, 193 (1989)
16. A. Djouadi, T. Köhler, M. Spira, J. Tutas, Z. Phys. C 46679 (1990)
17. The H1 Collaboration, C. Adloff et al., DESY 99-107, accepted for publication in Eur. Phys. J. C
18. The ZEUS Collaboration, J. Breitweg et al., Eur. Phys. J. C **11**, 427 (1999)
19. The H1 Collaboration, EPS HEP'99 paper #157b
20. The ZEUS Collaboration, EPS HEP'99 paper #549
21. T. Plehn, H. Spiesberger, M. Spira, P.M. Zerwas, Z. Phys. C **74**, 611 (1997)
22. The ZEUS Collaboration, J. Breitweg et al., Eur. Phys. J. C **12**, 411 (2000); The ZEUS Collaboration, EPS HEP'99 paper #558
23. The ZEUS Collaboration, J. Breitweg et al., Eur. Phys. J. C **16**, 253 (2000)
24. The H1 Collaboration, C. Adloff et al., Eur. Phys. J. C **11**, 447 (1999); DESY 00-027, submitted to Phys. Lett. B
25. The ALEPH Collaboration, CERN-EP/99-042; ALEPH-99-018; ALEPH-99-077; ALEPH-2000-025
26. The DELPHI Collaboration, CERN-EP/99-05; DELPHI 99-135; DELPHI 99-138
27. The L3 Collaboration, Phys. Lett. B **370**, 195 (1996); B **407**, 361 (1997); L3-Note-2227; L3-Note-2304; L3-Note-2398; L3-Note-2440; L3-Note-2500
28. The OPAL Collaboration, Eur. Phys. J. C **2**, 441 (1999); C **6**, 1 (1999); CERN-EP/99-097; OPAL-PN-420; OPAL-PN-424
29. LEP Electroweak Working Group, C. Geweniger et al, LEP2FF/00-01
30. The CDF Collaboration, F. Abe et al., Phys. Rev. Lett. **79**, 2198 (1997); Phys. Rev. D **59**, 052002 (1999)
31. The DØ Collaboration, Fermilab-CONF-98-273-E; Fermilab-PUB-98-391-E
32. The DØ Collaboration, B. Abbott et al., Phys. Rev. Lett. **79**, 4321 (1997); **80**, 2051 (1998)
33. The CDF Collaboration, F. Abe et al., Phys. Rev. Lett. **79**, 4327 (1997)
34. M. Krämer, T. Plehn, M. Spira, P.M. Zerwas, Phys. Rev. Lett. **79**, 341 (1997)
35. C. Grosso-Pilcher, G. Landsberg, M. Paterno, hep-ex/9810015
36. J. Blümlein, E. Boos, A. Kryukov, Z. Phys. C **76**, 137 (1997)
37. The DØ Collaboration, B. Abbott et al., A search for first generation vector leptoquarks, contribution to ICHEP'98
38. Y. Prescott et al., Phys. Lett. B **84**, 524 (1979); K. Hagiwara, D. Haidt, C.S. Kim, S. Matsumoto, Z. Phys. C **64**, 559 (1994); Erratum: C **68**, 352 (1995)
39. P.A. Souder et al., Phys. Rev. Lett. **65**, 694 (1990)
40. W. Heil et al., Nucl. Phys. B **327**, 1 (1989)
41. G. Altarelli, G.F. Giudice, M.L. Mangano, Nucl. Phys. B **506**, 29 (1997)
42. K. Hagiwara, S. Matsumoto, Phys. Lett. B **424**, 362 (1998); Erratum: K. Hagiwara, private communication
43. Particle Data Group, C. Caso et al., Eur. Phys. J. C **3**, 1 (1998); Particle Data Group, C. Caso et al., 1999; partial update for the 2000 edition available at http://pdg.lbl.gov/
44. W.J. Marciano, A. Sirlin, Phys. Rev. Lett. **71**, 3629 (1993); M. Finkemeier, Phys. Lett. B **387**, 391 (1996)
45. A. Derevianko, hep-ph 0005274

[8] Since July 1999 HERA scatters 27.5 GeV positrons on 920 GeV protons resulting in the center-of-mass energy $s^{1/2} = 318$ GeV. The currently available HERA e^+p data were collected in the years 1994–1997 with a proton beam energy of 820 GeV, corresponding to $s^{1/2} = 300$ GeV